

# Decoding quantum criticalities from fermionic/parafermionic topological states

Zi-Qi Wang<sup>1</sup>, Guo-Yi Zhu<sup>1</sup>, and Guang-Ming Zhang<sup>1,2</sup>

<sup>1</sup>State Key Laboratory of Low-Dimensional Quantum Physics and

Department of Physics, Tsinghua University, Beijing 100084, China.

<sup>2</sup>Collaborative Innovation Center of Quantum Matter, Beijing 100084, China.

(Dated: July 21, 2022)

In the Fock representation, we propose the generalized matrix product states to describe one-dimensional topological phases of fermions/parafermions. The defining feature of these topological phases is the presence of Majorana/parafermion zero modes localized at the edges. It is shown that the single-block bipartite entanglement spectrum and its entanglement Hamiltonian are described by the effective coupling between two edge quasiparticles. Furthermore, we demonstrate that sublattice bulk bipartition can create an extensive number of edge quasiparticles in the reduced subsystem, and the symmetric couplings between the nearest neighbor edge quasiparticles lead to the critical entanglement spectra, characterizing the topological phase transitions from the fermionic/parafermionic topological phases to its adjacent trivial phase. The corresponding entanglement Hamiltonians for the critical entanglement spectra can also be derived.

*Introduction.*- Topological phases of matter have been the subject of intense interest in condensed matter physics and quantum information science, because their anyonic low-energy excitations have potential use for fault-tolerant quantum computation. In a seminal paper, Li and Haldane[1] introduced the entanglement spectrum (ES) from the eigenvalues of the reduced density matrix upon tracing out a subsystem, and found that the low-lying excitations bear a remarkable similarity to the physical edge spectrum of the topological state[2–5]. It was further argued that the quantum criticality characterizing the phase transition from a topological phase to its adjacent trivial phase can also be decoded from the topological ground state wave function even far from critical point[6–10].

The simplest example of topological phases is the Haldane gapped phase of spin-1 chain[11]. With the spin-1 Affleck-Kennedy-Lieb-Tasaki matrix product state (MPS) wave function[12], it has been demonstrated that[8, 10] the *symmetric bulk* bipartition, in which the spin chain is divided into two subsystems both including the same blocks, creates an extensive number of spin-1/2 edge spins in the reduced subsystem. As long as each block includes even number of sites, the resulting ES is quantum critical in the thermodynamic limit, characterized by the SU(2) level-1 Wess-Zumino-Witten conformal field theory (CFT). The corresponding entanglement Hamiltonian (EH) can be expressed by the spin-1/2 edge degrees of freedom[10].

Actually the fractionalized edge quasiparticles (Majorana fermions/parafermions) with non-abelian statistics are also the defining property of one-dimensional fermionic/parafermionic topological phases[13–15]. Recently the fermionic MPS have been proposed by using the basis of the fermion number parity[16, 17]. When this fermion parity is generalized to the parafermion charge, the MPS for topological phases with  $\mathbb{Z}_N$  parafermions can be constructed[18, 19]. However, these

fermionic/parafermionic MPS represent the fixed-point wave functions of the topological phases with zero correlation length, so the quantum criticality can not be extracted from these wave functions[8, 10].

In this paper, we first introduce the generalized fermionic/parafermionic MPS wave functions with finite correlation length, maintaining the same properties as the fixed-point wave functions of the topological phases. Then we calculate the single-block bipartite ES and its EH, which are described by an effective coupling between two edge quasiparticles. What is more, we further prove that the sublattice bulk bipartition is an effective way to create an extensive number of edge quasiparticles in the reduced subsystem, and the symmetric couplings between the nearest neighbor edge quasiparticles of the subsystem can give rise to the gapless ES. For the  $\mathbb{Z}_2$  fermionic and  $\mathbb{Z}_3$  parafermionic cases, we carry out the detailed numerical studies for the ES. With the analysis of finite-size scaling, the resulting ES become quantum critical in the thermodynamic limit, characterizing the topological phase transitions from the fermionic/parafermionic topological phases to its adjacent trivial phase. We also derive the corresponding EH for the critical ES.

*$\mathbb{Z}_N$  Parafermionic MPS.*- For fermionic topological phases, the  $\mathbb{Z}_2$  parity of particle number is intrinsic symmetry, and the corresponding local Hilbert space is decomposed into the odd and even parity sectors:  $\mathbb{H} = \mathbb{H}_0 \oplus \mathbb{H}_1$ . When this super vector space is generalized to  $\mathbb{Z}_N$  charge sectors:  $\mathbb{H} = \mathbb{H}_0 \oplus \mathbb{H}_1 \oplus \dots \oplus \mathbb{H}_{N-1}$ , they can describe the  $\mathbb{Z}_N$  parafermions satisfying the following relations

$$\chi_l^N = 1; \quad \chi_l^\dagger = \chi_l^{N-1}; \quad \chi_l \chi_m = e^{i\frac{2\pi}{N}} \chi_m \chi_l, \quad (1)$$

for  $l < m$ . Unlike the boson/spin systems, the parafermionic many-body states are formed by an  $\mathbb{Z}_N$ -graded tensor products of the single-particle states:

$$|k_1, k_2, \dots, k_L\rangle = |k_1\rangle \otimes_g |k_2\rangle \otimes_g \dots \otimes_g |k_L\rangle, \quad (2)$$

where  $|k\rangle$  denotes the parafermion charge in the Fock representation[20]. Exchanging two nearest neighbor parafermion states are mathematically expressed by an isomorphism for the graded state vectors

$$\begin{aligned}\mathcal{F}\left(|k_l\rangle \otimes_g |j_m\rangle\right) &= e^{i\frac{2\pi}{N}k_l j_m} |j_m\rangle \otimes_g |k_l\rangle, \\ \mathcal{F}\left(\langle k_l| \otimes_g |j_m\rangle\right) &= e^{-i\frac{2\pi}{N}k_l j_m} |j_m\rangle \otimes_g \langle k_l|,\end{aligned}\quad (3)$$

where  $l < m$ , and the inner product can be defined by the contraction:

$$\mathcal{C}\left(\langle k_l| \otimes_g |j_m\rangle\right) = \langle k_l|j_m\rangle = \delta_{k_l-j_m}. \quad (4)$$

It should be noted that the operations of  $\mathcal{C}$  and  $\mathcal{F}$  commute each other, and the parafermion operators acting on the many-body parafermionic states follow as

$$\begin{aligned}\chi_{2j}|\dots k_j \dots\rangle &= -e^{i\frac{2\pi}{N}(\sum_{l\leq j} k_l - \frac{1}{2})} |\dots (k_j - 1)_{\text{mod } N} \dots\rangle, \\ \chi_{2j-1}|\dots k_j \dots\rangle &= e^{i\frac{2\pi}{N}\sum_{l<j} k_l} |\dots (k_j - 1)_{\text{mod } N} \dots\rangle,\end{aligned}\quad (5)$$

where the phase strings arise from the non-local commutation relation of parafermions.

In general, the parafermionic MPS can be constructed as[18, 19]:

$$|\Psi\rangle = \sum_{k_1, \dots, k_L} v_L^T A^{[k_1]} \dots A^{[k_L]} v_R |k_1 \dots k_L\rangle, \quad (6)$$

where  $v_L^T$  and  $v_R$  specify the boundary vectors. Each local site is associated with a graded tensor product of vectors:

$$\hat{\mathbf{A}} \equiv \sum_{\alpha\beta k} A_{\alpha\beta}^{[k]} |\alpha\rangle \otimes_g |k\rangle \otimes_g |\beta\rangle \quad (7)$$

where  $|\alpha\rangle$  and  $|\beta\rangle$  denote two virtual parafermionic vectors. Contraction of the virtual vectors ties the neighboring sites by maximally entangled bonds. As a general  $\mathbb{Z}_N$  parafermionic MPS for topological phases, we propose the local tensor with a tunable parameter  $\phi$  playing the chemical potential role:

$$A_{\alpha,\beta}^{[k]} = C e^{-k\phi/N} \delta_{\beta-\alpha-k \pmod{N}}, \quad (8)$$

where  $C$  is a normalization factor to be determined later. It should be emphasized that, when  $\phi = 0$ , the above MPS wave functions return to the fixed-point MPS forms[18, 19], maintaining the same topological properties. This is essentially due to the gauge symmetry  $\tau^\dagger A^{[k]} \tau = A^{[k]}$ , where  $\tau$  is the generator of the  $\mathbb{Z}_N$  group with its matrix element  $\tau_{\alpha,\beta} = \delta_{\alpha-\beta-1}$ . Actually, Eq.8 does not exhaust all possibilities, because there can be at most  $N - 1$  independent parameters controlling the relative distribution of the  $N$  physical channels on each lattice site. We also notice that, when  $N = 2$ , the above MPS wave function is reduced to the exact ground states

of the interacting Kitaev Majorana fermion chain[21], while for  $N = 3$ , it is equivalent to the exact solution to a specific  $\mathbb{Z}_3$  parafermion chain[22].

With the MPS wave functions, the generic correlator  $\langle \psi | \hat{O}_i \hat{O}_j | \psi \rangle$  can be cast into a tensor network, which involves a consecutive mapping through the transfer matrix:

$$\mathbb{E}_{(\alpha\alpha'),(\beta\beta')} = \sum_k A_{\alpha,\beta}^{[k]} \bar{A}_{\alpha'\beta'}^{[k]}. \quad (9)$$

Unlike the bosonic MPS, the calculation of the correlator involves additional phase factor counting the total charge between site  $i$  and  $j$  due to the parafermion commutation. Nevertheless, this seemingly non-local phase can be attributed to a local charge detector deposited on the virtual bonds at sites  $i$  and  $j$ . Diagonalizing the transfer matrix, we obtain the eigenvalue spectrum  $\lambda_n = |\lambda_n| e^{i\theta_n}$  ( $n = 0, 1, 2, \dots, N-1$ ), where

$$|\lambda_n|^2 = 1 + \frac{\sin^2 \frac{\pi n}{N}}{\sinh^2 \frac{\phi}{N}}, \quad \tan \theta_n = \frac{\sin \frac{2\pi n}{N}}{e^{2\phi/N} - \cos \frac{2\pi n}{N}}, \quad (10)$$

and each eigenvalue has  $N$ -fold degeneracy, because the transfer matrix inherits the local gauge symmetry as the signature of the topological nontriviality:  $(1 \otimes \tau^\dagger) \mathbb{E} (1 \otimes \tau) = \mathbb{E}$ . The eigenvectors within the degenerate subspace are therefore related by  $(1 \otimes \tau)$  or  $(\tau \otimes 1)$ . Among the  $N$  eigenvectors of each eigenvalue, one has diagonal form

$$(R_n/L_n)_{\alpha,\alpha'} = \frac{1}{\sqrt{N}} e^{\pm i\frac{2\pi}{N}n\alpha} \delta_{\alpha'-\alpha}. \quad (11)$$

The normalization factor  $C$  can be chosen to make  $\lambda_0 = 1$ , and the other eigenvalues  $|\lambda_n| \leq 1$  with  $\lambda_n = \lambda_{N-n}$ . Since the correlation function  $\langle \psi | \hat{O}_i \hat{O}_j | \psi \rangle - \langle \psi | \hat{O}_i | \psi \rangle \langle \psi | \hat{O}_j | \psi \rangle \propto \lambda_1^{|j-i|}$ , the correlation length  $\zeta$  is determined:

$$\zeta^{-1} = \frac{1}{2} \ln \left( 1 + \frac{\sin^2 \frac{\pi}{N}}{\sinh^2 \frac{\phi}{N}} \right). \quad (12)$$

*Single-block ES.* - To study the edge excitations of the topological phases, we divide the system into one block of  $l$  sites ( $l \gg \zeta$ ) and its complements (Fig. 1a), and then block the local matrices of  $l$ -sites altogether as a matrix  $\tilde{A}_{\alpha\beta}^{\{k_i\}}$ . After performing the singular value decomposition  $\tilde{A} = USV^\dagger$ , we find that  $U_{(\alpha\beta),p} = \delta_{\beta-\alpha-p}/\sqrt{N}$  assembles the virtual modes to the effective degrees of freedom  $p$  and  $V$  as an isometry transformation maps the block physical degrees of freedom  $\{k_i\}$  to the effective edge degrees of freedom  $p$ . The singular values of the diagonal matrix  $S$  are given by

$$s_p = \left( \sum_{n=0}^{N-1} e^{i(\frac{2\pi}{N}np + l\theta_n)} |\lambda_n|^l \right)^{1/2}, \quad p = 1, 2, \dots, N. \quad (13)$$

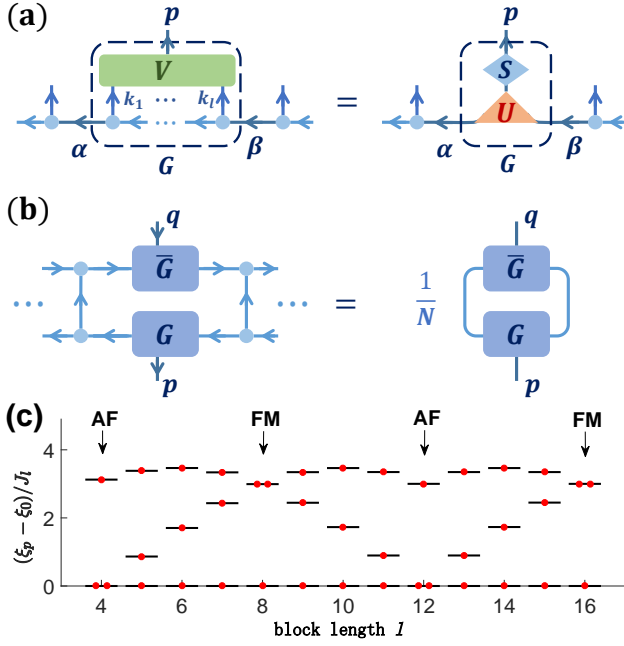


FIG. 1: (a) Applying an isometry to the block of  $l$  sites. (b) The reduced density operator of the block. (c) The single-block ES for  $\mathbb{Z}_3$  parafermionic MPS with  $\phi \simeq 1.5076$ . The ES structure shows a periodicity with respect to the block length  $l$ : ferromagnetic and anti-ferromagnetic couplings between two edge parafermions.

So an effective block tensor can be defined by  $G_{\alpha\beta}^{[p]} = (US)_{(\alpha\beta),p} = s_p \delta_{\beta-\alpha-p} / \sqrt{N}$ , and the effective reduced density matrix is given by  $\tilde{\rho}_r \equiv V^\dagger \rho_r V \equiv e^{-H_b}$ , where  $H_b$  faithfully characterizes the physics of the reduced subsystem. For the sufficient long complements of the block (Fig. 1b),  $\tilde{\rho}_r$  is simplified as

$$(\tilde{\rho}_r)_{p,q} = \text{tr} \left[ G^{[p]} R_0 \left( G^{[q]} \right)^\dagger L_0^\dagger \right] = \frac{1}{N} s_p^2 \delta_{p-q}. \quad (14)$$

Therefore, the single-block ES given by the eigenvalues of  $H_{\text{ent}}$  is obtained as

$$\xi_p = -\ln \left( \frac{1}{N} \sum_{n=0}^{N-1} e^{i(\frac{2\pi}{N} np + l\theta_n)} |\lambda_n|^l \right). \quad (15)$$

It should be noticed that the entanglement levels subtracted the lowest one depend exponentially on the block length  $l$ :  $\xi_p - \xi_0 \propto e^{-l/\zeta} \equiv J_l$ . Thanks to the finite correlation length of the generalized wave functions, the effective coupling between two edges helps us to reveal the structure of the ES.

For the  $\mathbb{Z}_2$  case, the single-block ES has two entanglement levels with different parities, and the spectral gap is simply proportional to  $J_l$ . Up to the leading order of  $J_l$ , the corresponding EH is given by  $H_b = -iJ_l \gamma_1 \gamma_2 + \ln 2$ , where  $\gamma_1$  and  $\gamma_2$  are the two edge Majorana fermions. For  $N \geq 3$ , the single-block ES exhibits a richer structure as a function of block length with an asymptotic

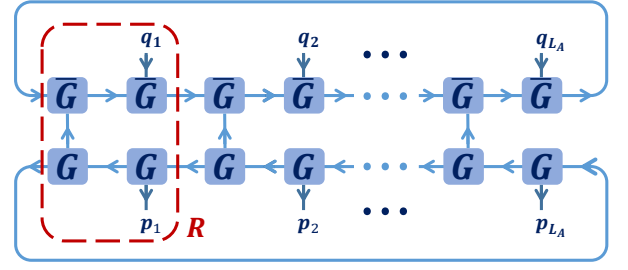


FIG. 2: A graphical tensor-network of the reduced density operator with the repeating tensor  $R$  under the symmetric bulk bipartition. The arrows signify the tensor-network carrying parafermionic statistics.

periodicity of  $2\pi/N$ :  $\xi_p \simeq \ln N - 2J_l \cos\left(\frac{2\pi p}{N} + l\theta_1\right)$ . So the corresponding EH can be found

$$\hat{H}_b \simeq \left[ J_l e^{i(l\theta_1 - \frac{\pi}{N})} \psi_1^\dagger \psi_2 + h.c. \right] + \ln N, \quad (16)$$

which describes the effective coupling between the two edge parafermions  $\psi_1$  and  $\psi_2$ . In Fig. 1c, the scaled spectrum for the  $\mathbb{Z}_3$  case has shown the periodicity of the level structure from the coupling phase cycling with the block length. In particular,  $l\theta_1 = 2k\pi$  and  $l\theta_1 = (2k+1)\pi$  ( $k$  an integer) correspond to the "ferromagnetic" and "anti-ferromagnetic" couplings, respectively. The former has a non-degenerate lowest level and two-fold degenerate excited level, while the latter displays the inverse order. When  $\phi = 0$ ,  $\zeta = 0$  and  $J_l = 0$ , two edge parafermions are completely decoupled, and the ES becomes single level with a three-fold degeneracy.

*Reduced subsystem under symmetric bulk bipartition.*— In order to create an extensive number of edge Majorana/parafermions in the reduced subsystem for a topological ground state, we have to divide the system into two sublattices with the block lengths of  $l_A$  and  $l_B$ , respectively[8, 10]. Depending on the relative length of  $l_A$  and  $l_B$ , the reduced subsystem A can accommodate both the topological phase and trivial phase: when  $l_B$  is relatively small, the reduced subsystem A is essentially the same phase as the original topological phase, while it becomes a trivial dimerized phase for a relatively small  $l_A$ . If the relative block lengths  $l_A$  and  $l_B$  are gradually varied, the symmetric bulk bipartition ( $l_A = l_B = l$ ) approaches, and the reduced subsystem A reaches at quantum critical point between the topological phase and the trivial phase. It is known that the  $\mathbb{Z}_2$  topological phase is connected to the trivial phase by the translation of Majorana fermions or the duality transformation, so the quantum criticality can be obtained by the symmetric bulk bipartition[13, 14]. For the general  $\mathbb{Z}_N$  parafermionic topological phases, however, there may exist more than one critical points.

Let us first group every  $l$  sites together and apply the isometry transformation  $V$  to form the block tensor  $G$ .

By tracing out the blocks of the subsystem B, the reduced density operator is obtained in the form of tensor network, as shown in Fig. 2. However, the tracing process is not straightforward, because it needs permuting the parafermionic variables which would inevitably result in non-local phases. Nevertheless, this can be circumvented by redistributing the non-local phase into each block locally at the cost of introducing additional bond that tracks and records the total charge of all the parafermions to the left of a given block[23]. Then the reduced density operator turns into the conventional form of matrix product operator,

$$(\rho_A)_{p,q} = C' \text{tr} \left( R^{[p_1, q_1]} \dots R^{[p_{L_A}, q_{L_A}]} \right)_{l=r=0}, \quad (17)$$

with the repeating tensor

$$R_{(\alpha l \gamma), (\beta r \delta)}^{[p, q]} = \frac{s_p s_\beta^{2-\alpha-p} s_q}{N^2} \delta_{\beta-\delta-\alpha+l} \delta_{r-l-p+q} e^{i \frac{2\pi}{N} (\beta-\alpha-p)l},$$

where  $C'$  is the normalization factor,  $\alpha, \beta, \gamma, \delta$  denote the virtual bonds, and  $l, r$  inputs/outputs the accumulated charge to the left of the repeating tensor, respectively. So the ES can be numerically calculated as the eigenvalues of  $H_{\text{ent}} = -\ln \hat{\rho}_A$ .

*Numerical results.*- Now we would like to present the numerical results for the two simplest cases. For the  $\mathbb{Z}_2$  fermionic MPS with  $\phi = 2$ , we exactly calculate the ES under symmetric bulk bipartition with the block length  $l = 5$ , and the numerical results are displayed in Fig. 3a. The analysis of finite-size scaling for the first two excited levels are shown in Fig. 3b, indicating that the ES is quantum critical in the thermodynamic limit. Further studies on the entanglement entropy of the lowest entanglement state allow us to extract the central charge  $c$  of the quantum criticality by fitting the Calabrese-Cardy formula[24]

$$S_V(x, L_A) = \frac{c}{3} \ln \left[ \frac{2L_A}{\pi} \sin \left( \frac{\pi x}{L_A} \right) \right] + \text{const.}, \quad (18)$$

where  $x$  is the length chosen from the  $L_A$  reduced subsystem. As shown in Fig. 3c, the central charge  $c \simeq 1/2$  uniquely points to the one-dimensional Ising CFT, which characterize the quantum critical point separating the  $\mathbb{Z}_2$  topological phase from trivial phase of the Kitaev Majorana fermion chain[13, 14].

In contrast to the  $\mathbb{Z}_2$  case, there are more than one quantum critical points for the  $\mathbb{Z}_3$  parafermionic MPS, depending on the block length  $l$ . Two important cases correspond to  $l\theta_1 = 2k\pi$  and  $(2k+1)\pi$ . In the second case, an even-odd dependence on the subsystem size demands us to consider the even subsystem sizes only. Their ES scaled by  $J_l$  are shown in Fig. 4a and 4d, respectively. From the analysis of finite-size scaling of two lowest excited levels (Fig. 4b and 4e), both ES are quantum critical in the thermodynamic limit.

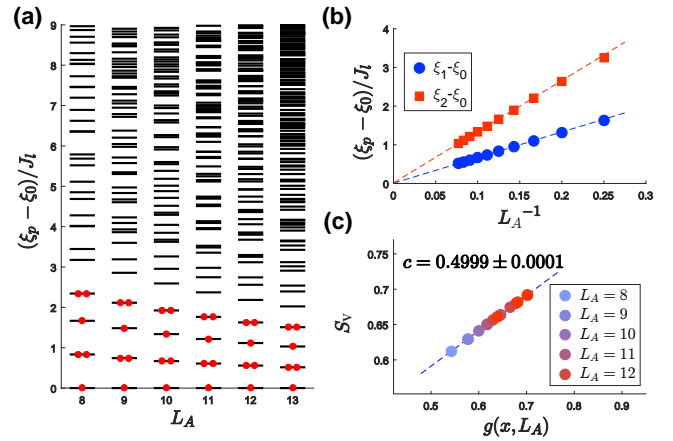


FIG. 3: For the  $\mathbb{Z}_2$  fermionic topological state with  $\phi = 2$  under a symmetric bulk bipartition. (a) ES for different  $L_A$  as the effective lengths of the reduced subsystem with the block length  $l = 5$ . (b) The finite-size scaling of the lowest two excited levels. (c) The entanglement entropy  $S_V$  of the lowest entanglement level is fitted with  $g(x, L_A) = \frac{1}{3} \ln [2L_A/\pi \sin(\pi x/L_A)]$ .

Similarly, the entanglement entropy of the lowest states (Fig. 4c and 4f) yield that the  $\mathbb{Z}_3$  parafermionic CFT with central charge  $c \simeq 4/5$  is obtained in the "ferromagnetic" couplings between the nearest neighbor edge parafermions[25], while the central charge is found to be  $c \simeq 1$  for the "anti-ferromagnetic" couplings between the nearest neighbor edge parafermions, consistent with the  $U(1)$  level-6 CFT[26, 27]. The former criticality is associated to the phase transition from the  $\mathbb{Z}_3$  topological phase to the trivial phase, while the latter criticality is related to the incommensurate phase adjacent to the  $\mathbb{Z}_3$  topological phase[28]. So we have decoded a family of quantum critical theories from the  $\mathbb{Z}_3$  topological MPS wave function.

*Effective critical Hamiltonians.*- In order to analytically deduce the EH for the reduced subsystem, the reduced density operator  $\hat{\rho}_A$  has to be expressed in terms of the edge parafermions of each block by using the relations Eq.(5). Under the periodic boundary condition,  $\hat{\rho}_A$  can be decomposed into

$$\hat{\rho}_A = \left( \prod_{j=1}^{L_A} \hat{S}_i \right) \left( \prod_{j=1}^{L_A} \hat{T}_i \right) \left( \prod_{j=1}^{L_A} \hat{S}_i \right), \quad (19)$$

where  $\hat{S}_j = \left[ \sum_{m=0}^{N-1} \lambda_m^l \left( e^{-i\pi(\frac{1}{N}+1)} \psi_{2j-1}^\dagger \psi_{2j} \right)^m \right]^{1/2}$  is the operator of the diagonal singular matrix of each block, describing the coupling between the edge parafermions from the same block, and  $\hat{T}_j = \sum_{m=0}^{N-1} \lambda_m^l \left( e^{-i\pi(\frac{1}{N}+1)} \psi_{2j}^\dagger \psi_{2j+1} \right)^m$  denotes the coupling between the edge parafermions from the adjacent blocks. Since the coupling amplitude  $J_l$  decays exponentially with the correlation length of the topological MPS states,



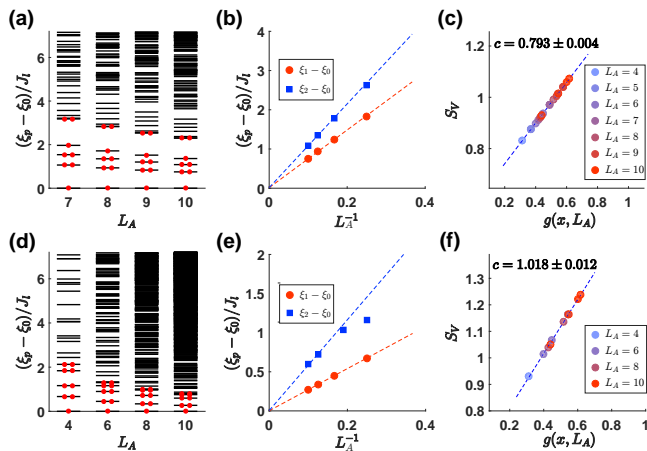


FIG. 4: For  $\mathbb{Z}_3$  parafermionic MPS wave function with  $\phi \simeq 1.5076$ . The block length is chosen as  $l = 12$  in the top panel, while  $l = 24$  in the low panel. (a), (d) The ES for different subsystem lengths  $L_A$ . (b), (e) The finite-size scaling of the lowest two excited levels. (c), (f) The entanglement entropy  $S_V$  of the lowest entanglement level is fitted with  $g(x, L_A) = \frac{1}{3} \ln [2L_A/\pi \sin(\pi x/L_A)]$ .

we have the privilege to expand  $\ln \hat{\rho}_A$  in the limit  $l \gg \zeta$ . The leading order of  $J_l$  gives rise to the dominant contribution of the EH,

$$\hat{H}_{\text{ent}} \simeq J_l \sum_{j=1}^{2L_A} \left[ e^{i(\theta_1 - \frac{\pi}{N})} \psi_j^\dagger \psi_{j+1} + h.c. \right] + L_A \ln N, \quad (20)$$

which faithfully describes the quantum criticality of the reduced subsystem. It is true that  $\hat{H}_{\text{ent}}$  corresponds to the critical model Hamiltonians in the  $\mathbb{Z}_2$  and  $\mathbb{Z}_3$  cases, respectively[13–15]. Therefore, we have not only extracted the complete family of the topological quantum critical theories encoded in the  $\mathbb{Z}_N$  parafermionic topological states, but also derived the corresponding critical lattice model Hamiltonians, whose coupling strengths can be well controlled by the block length.

*Conclusion.*— Based on the generalized MPS wave functions of topological phases, we have demonstrated that sublattice bulk bipartition creates an extensive number of edge quasiparticles in the reduced subsystem, and the symmetric couplings between the nearest neighbor edge quasiparticles give rise to the critical ES, characterizing the topological phase transitions from the fermionic/parafermionic topological phases to its adjacent trivial phases.

*Acknowledgment.*— The authors would like to thank W. T. Xu for his stimulating discussions and acknowledge

the support of National Key Research and Development Program of China (No.2017YFA0302902).

- [1] H. Li and F. D. M. Haldane, Phys. Rev. Lett. **101**, 010504 (2008).
- [2] J. I. Cirac, D. Poilblanc, N. Schuch and F. Verstraete, Phys. Rev. B **83**, 245134 (2011).
- [3] A. Chandran, M. Hermanns, N. Regnault and B. A. Bernevig, Phys. Rev. B **84**, 205136 (2011).
- [4] X. L. Qi, H. Katsura and A. W. W. Ludwig, Phys. Rev. Lett. **108**, 196402 (2012).
- [5] F. Pollmann, A. M. Turner, E. Berg and M. Oshikawa, Phys. Rev. B **81**, 064439 (2010).
- [6] T. H. Hsieh and L. Fu, Phys. Rev. Lett. **113**, 106801 (2014).
- [7] Q. Zhu, X. Wan, and G. M. Zhang, Phys. Rev. B **90**, 235134 (2014).
- [8] W. J. Rao, X. Wan and G. M. Zhang, Phys. Rev. B **90**, 075151 (2014).
- [9] T. H. Hsieh, L. Fu and X. L. Qi, Phys. Rev. B **90**, 085137 (2014).
- [10] W. J. Rao, G. M. Zhang, and K. Yang, Phys. Rev. B **93**, 115125 (2016).
- [11] F. D. M. Haldane, Phys. Lett. **93A**, 464 (1983).
- [12] I. Affleck, T. Kennedy, E. H. Lieb and H. Tasaki, Phys. Rev. Lett. **59**, 799 (1987).
- [13] A. Y. Kitaev, Physics-Uspekhi **44**, no. 10S, 131 (2001).
- [14] L. Fidkowski, A. Kitaev, Phys. Rev. B **83**, 075103 (2011).
- [15] P. Fendley, J. Statistical Mechanics: Theory and Experiment 2012, P11020.
- [16] N. Bultinck, D. J. Williamson, J. Haegeman, and F. Verstraete, Phys. Rev. B **95**, 075108 (2017).
- [17] A. Kapustin, A. Turzillo, and M. You, arXiv:1610.10075.
- [18] W. T. Xu and G. M. Zhang, Phys. Rev. B **95**, 195122 (2017).
- [19] W. T. Xu and G. M. Zhang, Phys. Rev. B **97**, 035160 (2018).
- [20] E. Cobanera and G. Ortiz, Phys. Rev. A **89**, 012328 (2014).
- [21] H. Katsura, D. Schuricht, and M. Takahashi, Phys. Rev. B **92**, 115137 (2015).
- [22] F. Iemini, C. Mora, and L. Mazza, Phys. Rev. Lett. **118**, 170402 (2017).
- [23] C. V. Kraus, N. Schuch, F. Verstraete, and J. I. Cirac, Phys. Rev. A **81**, 052338 (2010).
- [24] P. Calabrese and J. Cardy, J. Stat. Mech. (2004) P06002.
- [25] V. S. Dotsenko, Nucl. Phys. B **235**, 54 (1984).
- [26] R. Kedem and B. M. McCoy, J. Stat. Phys. **71**, 865 (1993).
- [27] W. Li, S. Yang, H. H. Tu, and M. Cheng, Phys. Rev. B **91**, 115133 (2015).
- [28] Y. Zhuang, H. J. Changlani, N. M. Tubman, and T. L. Hughes, Phys. Rev. B **92**, 035154 (2015).